Nuclease-resistant nucleic acid ligands to vascular permeability factor/vascular endothelial growth factor

Louis S Green, Derek Jellinek, Carol Bell, Laurie A Beebe, Bruce D Feistner, Stanley C Gill, Fiona M Jucker and Nebojša Janjić*

NeXstar Pharmaceuticals, 2860 Wilderness Place, Boulder, Colorado 80301, USA

Background: Vascular permeability factor/vascular endothelial growth factor (VPF/VEGF) is a potent inducer of new blood vessel growth (angiogenesis) that contributes to the pathology of many angiogenesis-associated disease states such as psoriasis, rheumatoid arthritis and cancer. Few molecular entities capable of binding to VPF/VEGF with high affinity and specificity have been described to date.

Results: Nuclease-resistant 2'-amino-2'-deoxypyrimidine nucleotide RNA (2'-aminopyrimidine RNA) ligands that bind to VPF/VEGF with high affinity have been identified by iterative rounds of affinity-selection/amplification from two independent random libraries. The sequence information that confers high affinity binding to VPF/VEGF is contained in a contiguous stretch of 24 nucleotides, 5'-*CCCU*GA*U*GG*U*AGA*C*-GCCGGGG*U*G-3' (2'-aminopyrimidine nucleotides are designated with italic letters). Of the 14 ribopurines in this minimal ligand, 10 can be substituted with the corresponding 2'-O-methylpurine nucleotides without a reduction in binding affinity to VPF/VEGF. In fact, the 2'-O-methyl substitution at permissive positions leads to a ~17-fold improvement in the binding affinity to VPF/VEGF. The higher affinity results from the reduction in the dissociation rate constant of the 2'-O-methyl-substituted RNA ligand from the protein compared to the unsubstituted ligand. The 2'-O-methyl-substituted minimal ligand, which folds into a bulged hairpin motif, is also more thermally stable than the unsubstituted ligand. Nuclease resistance of the ligand is further improved by the 2'-O-methyl substitutions and the addition of short phosphorothioate caps to the 3'- and 5'-ends.

Conclusions: We have used the SELEX (systematic evolution of ligands by exponential enrichment) process in conjunction with post-SELEX modifications to define a highly nuclease-resistant oligonucleotide that binds to VPF/VEGF with high affinity and specificity.

Chemistry & Biology October 1995, **2**:683–695

Key words: angiogenesis, 2'-amino-2'-deoxypyrimidine nucleotide RNA, combinatorial libraries, *in vitro* evolution, nuclease-resistant oligonucleotides

Introduction

Growth and metastasis of malignancies is dependent on the development of new blood vessels, or angiogenesis [1,2]. In addition to other abnormal features, tumor-associated vasculature is considerably more permeable to plasma fluid and protein than the vasculature of normal tissues [3,4]. This observation has led to the discovery of vascular permeability factor (VPF) as a tumor-secreted protein that in very low amounts induces a rapid increase in vascular permeability independent of mast-cell degranulation or endothelial-cell damage [5–7]. Several groups have subsequently and independently isolated a growth factor from pituitary follicular [8,9] and glioma tumor cell conditioned media [10] that was selectively mitogenic for vascular endothelial cells; this protein was named vascular endothelial growth factor (VEGF) [8]. VPF and VEGF were soon shown to be encoded by the same gene, which gives rise to four protein isoforms (121-, 165-, 189- and 206-amino-acid species) as a result of alternative splicing of mRNA [11–14]. VPF/VEGF is a secreted N-glycosylated disulfide-linked homodimer that exerts its effects on endothelial cells by binding to tyrosine kinase receptors encoded by the flt and the flk-1/KDR genes [15–17].

The ability to produce and secrete VPF/VEGF is shared by many, if not most, tumor cells [5–7,10,18–22]. There is now considerable evidence that VPF/VEGF secreted by tumors acts in a paracrine manner on the adjacent endothelial cells [23,24]. Recently, direct evidence that VPF/VEGF contributes to the growth of solid tumors has been obtained: neutralizing antibodies to VPF/VEGF [19] and a transfected dominant-negative VPF/VEGF receptor [25] were found to inhibit the growth of xenografted human tumor cell lines in immunocompromized mice. Elevated levels of VPF/VEGF have also been found in sera of cancer patients [26].

Since disregulated proliferation of blood vessels contributes to the pathology of many other disease states including psoriasis, rheumatoid arthritis and retinopathies [2] in which VPF/VEGF may be important, there is a substantial impetus for the discovery of specific and potent ligands/antagonists of VPF/VEGF.

The ease with which nucleic acid libraries of enormous size can be generated and screened for molecules with unique functional properties has recently led to the emergence of the SELEX (systematic evolution of

*Corresponding author.

 ISSN 1074-5521

ligands by exponential enrichment) combinatorial chemistry process as one of the most efficient methods of discovering new therapeutic and diagnostic candidates. In the few years since the SELEX process was first described, a large number of nucleic acid sequences with unique binding or catalytic properties has been described (reviewed in [27,28]). The remarkable success of SELEX is a salient illustration of the diversity of molecular features embodied in random nucleic acid libraries. Recently, we and others have shown that SELEX is not confined to the use of natural RNA and DNA libraries [29–31]. With the understanding that the modifications in nucleic acids are acceptable as long as the substrate requirements of the relevant enzymes are met, various chemical moieties can be introduced with the aim of providing the libraries with an expanded repertoire of functional groups and/or of imparting increased nuclease resistance.

We have previously reported the use of the SELEX process to identify specific high affinity RNA ligands to VPF/VEGF from a random RNA library [32]. In this report, we describe the identification of nuclease-resistant modified RNA ligands to VPF/VEGF from two independent 2'-amino-2'-deoxypyrimidine nucleotide RNA (2'-aminopyrimidine RNA) libraries. We demonstrate that the stability in biological fluids as well as the affinity and specificity of the initial lead compound for VPF/VEGF can be further improved by post-SELEX modifications.

Results

Selection of high-affinity ligands

High affinity 2'-aminopyrimidine RNA ligands to VPF/VEGF were selected from two random libraries (A and B) in independent SELEX experiments. In these libraries, randomized regions of length 30 and 50 were flanked by different fixed-sequence regions (see Materials and methods). The initial affinity selections in both SELEX experiments were performed with ≈6 x 10^{14} RNA molecules (1 nmol). After 11 rounds of affinity selection and amplification, the affinity improvement was about 100-fold (data not shown). We identified 79 unique-sequence isolates from the affinity-enriched pools (44 from library A and 35 from library B) as described [33]. These isolates were screened for VPF/VEGF binding by measuring the fraction of RNA bound to nitrocellulose filters at varying VPF/VEGF concentrations. Those that were retained efficiently on nitrocellulose filters in the absence of VPF/VEGF (36 clones) were not considered further. The remaining 43 ligands bound to VPF/VEGF with estimated dissociation constant (K_d) values ranging from 10^{-10} to 10^{-8} M; the random pool had a K_d value of ≈10^{-7} M. The high-affinity ligands to VPF/VEGF fall into several sequence families, typically containing isolates from both library A and library B. In the example shown in Figure 1, a 17-nucleotide stretch of highly conserved consensus primary structure is apparent. Extensive base-pairing covariation is observed between positions 1 and 23, 2 and 22, and 3 and 21; modest base-pairing covariation is seen between positions 4 and 20 (1 A–*U* and 5 *C*–G).

Dot-matrix analysis of the consensus secondary structure

To facilitate the detection of consensus secondary structures for nucleic acids, we have developed a method for simultaneously examining all possible base pairings in aligned sequence sets through the use of dot-matrix representation (Fig. 2) [34]. To produce the matrix, the sequence of the oligonucleotide is written as a column to define the x-axis and as a row to define the y-axis [35]. A symbol (dot) is placed in the matrix at all positions where base pairing occurs (G–*U* and *U*–G base pairs are allowed in this analysis). Double-helix (stem) regions are recognized as runs of adjacent bars perpendicular to the symmetry diagonal. By overlaying the aligned dot matrices of all ligands in the set, it is possible to identify positions where base pairing is conserved (shown in clear (background), blue and red, in order of

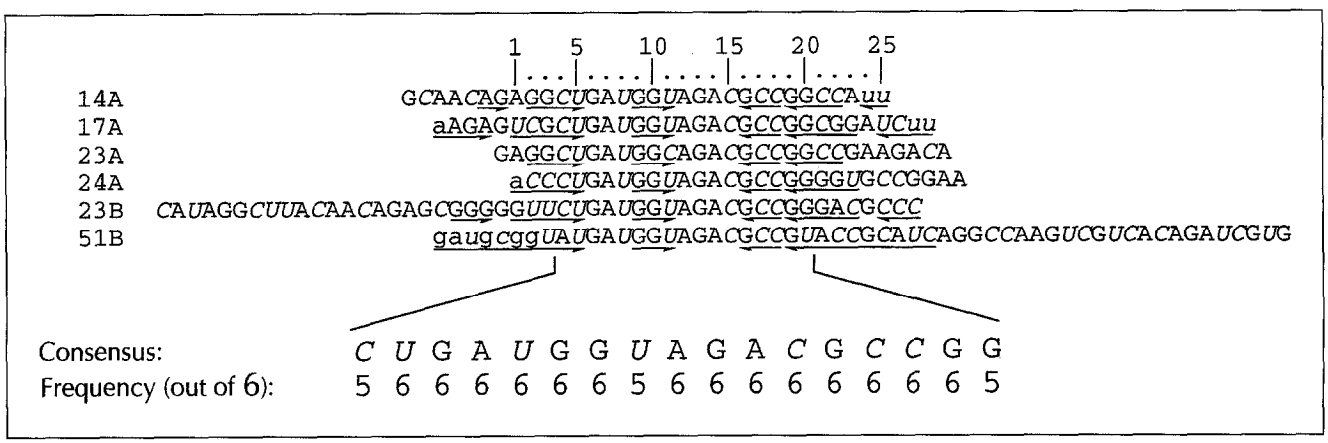

Fig. 1. Primary structures of a family of high affinity 2'-aminopyrimidine RNA ligands to VPF/VEGF. Aligned sequences isolated from the affinity-enriched RNA pools A and B are shown, depicting nucleotides in the evolved region (upper-case letters); also shown are nucleotides in the constant region (lower-case letters) that participate in the predicted consensus secondary structure formation (underline arrows). The 2'-aminopyrimidine nucleotides are shown in italic letters. The positions are numbered arbitrarily starting with the first shown nucleotide of ligand 24A. The consensus primary structure is shown below the sequence set, with the frequencies of occurrence for each of the conserved nucleotides.

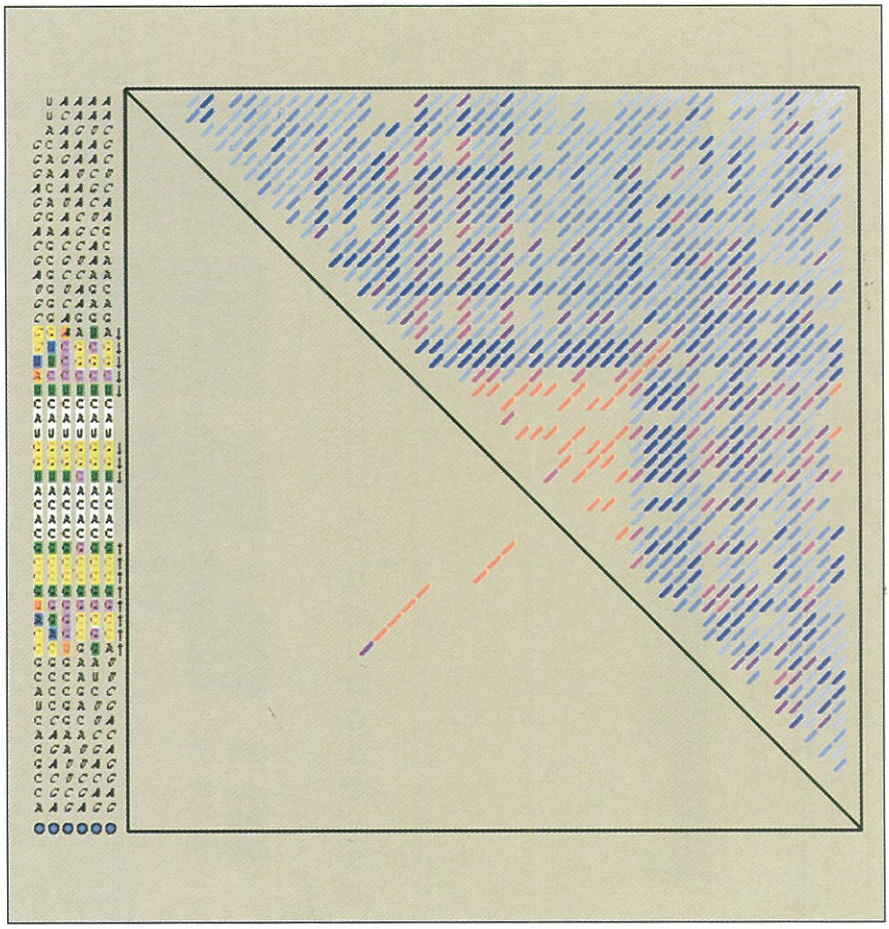

Fig. 2. Dot-matrix analysis to facilitate the detection of consensus secondary structure in nucleic acids, showing the consensus matrix analysis of the aligned sequence set in Figure 1. Each sequence in the set is written on two sides of a square (left and top, 5'-end at the top and left sides), and a symbol (diagonal bar) is placed inside the square at all positions where base pairing occurs (including G–*U* base pairs). For clarity, the aligned sequence set is only shown on the left side. Since each base pair in a sequence is represented twice, the matrix has a symmetry diagonal (top-left to bottom-right) that separates it into two triangles. Double-helical (stem) regions are recognized as runs of adjacent bars perpendicular to the symmetry diagonal. Positions within the matrix where base pairing occurs more than once are color-coded (red: base pairing occurs in all ligands (100 %) at that matrix position, purple: 75 %, blue: 50 %, light-blue: 25 %, and clear (background): 0 %). The upper-right triangle shows the entire (unfiltered) data set; the lower left triangle shows the filtered data set, displaying the most highly conserved secondary structure elements. The secondary structure depicted in the lower-left triangle corresponds to the region of the sequence set denoted by inverted vertical arrows; to show positions where base pairing covariation exists, corresponding colors are used to highlight the base pairs in this double-helical region.

increasing frequency). Since the information in the matrix is redundant, the top triangle is used for the unfiltered data set, while the lower triangle shows the most highly conserved and stable secondary structure elements. The identification of covariation between any two positions in a set is also possible by this method [34].

Minimal sequence determinations

The minimal sequence requirement for high affinity binding was determined for one of the best ligands (24A) in the sequence set shown in Figure 1, using partial alkaline hydrolysis followed be affinity selection [32] (see Fig. 3). The phosphodiester bonds adjacent (3') to the 2'-aminopyrimidine nucleotides are relatively resistant to alkaline hydrolysis [29,31,36], as manifested by the absence of bands at those positions. This allows sequence assignment in the absence of external markers from the pattern of purine nucleotides in the ligand, but also limits the resolution of the boundaries to the nearest purine nucleotide. A minimal ligand, 5'-A*CCCU*-GA*U*GG*U*AGA*C*G*C*C*G*GGG*U*G-3' (ligand NX-107; 2'-aminopyrimidine nucleotides are shown in italic letters), was inferred from these experiments. Binding affinities of the chemically synthesized minimal ligand NX-107 and its transcribed full length analog 24A for VPF/VEGF are essentially identical (data not shown).

Post-SELEX 2'-O-methyl substitutions at purines

There is now ample evidence that the 2'-aminopyrimidine RNA is substantially more resistant to degradation by nucleases in serum than is unmodified RNA [29,31,36]. To further reduce the number of positions that are susceptible to ribonuclease cleavage *in vivo*, we examined the extent to which the ribopurines in ligand NX-107 could be substituted with 2'-O-methyl (2'-OMe) purine nucleotides without compromising high-affinity binding to VPF/VEGF. As the phosphodiester bonds adjacent to 2'-OMe nucleotides are considerably more resistant to alkaline hydrolysis than those adjacent to ribonucleotides, we could examine the effect of the 2'-OMe substitution on binding at multiple positions simultaneously.

The 2'-OMe substitutions at the 14 purine nucleotide positions in ligand NX-107 were tested in four ligand pools, each with three to four mixed 2'-OMe/2'-OH positions (see Materials and methods). Resolution of the radiolabeled hydrolytic fragments of one of the partially 2'-OMe substituted pools (pool A) on denaturing polyacrylamide gels, before and after affinity selection, is shown in Figure 4. In the unselected lane, the bands that correspond to hydrolysis at positions 9, 12 and 14 are notably fainter compared to other purine nucleotide positions as a result of the partial 2'-OMe substitution. As noted above, the bands that correspond to hydrolysis at 2'-aminopyrimidine nucleotides are not observed. In the 7 nM and the 0.7 nM VPF/VEGF selection lanes, the A14 band is relatively more intense than in the unselected lane (compared, for example, to the G13 band). The A12 band, on the other hand, is less intense in the selected lanes than

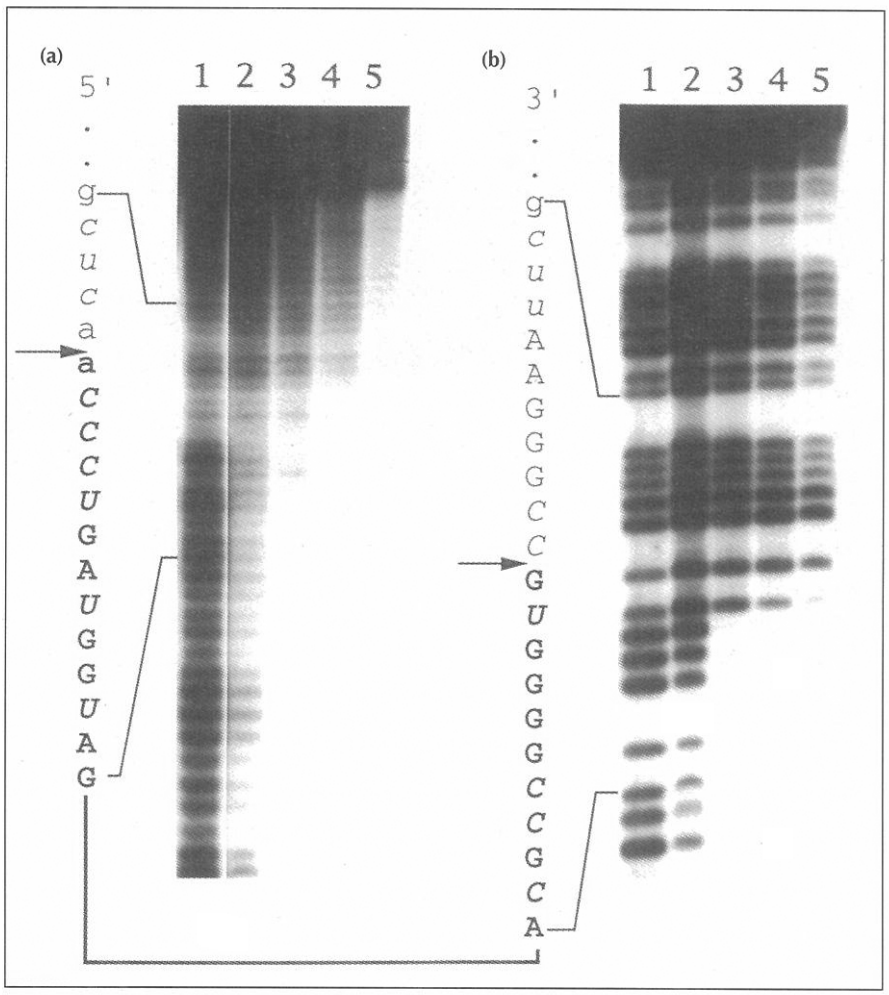

Fig. 3. Determination of the minimal sequence requirement for high-affinity binding of ligand 24A to VPF/VEGF. Partial alkaline hydrolysis fragments of **(a)** ^{32}P 3'- or **(b)** ^{32}P 5'-end-labeled ligand 24A were generated by incubating the RNA in 50 mM bicarbonate buffer, pH 9 for 15 min at 90 °C. The hydrolytic fragments were resolved on denaturing 8 % polyacrylamide gels. For the 5' boundary determined in (a), the partially hydrolyzed, 3'-labeled ligand (lane 1) was affinity selected with 170 nM (lane 2), 17 nM (lane 3), 1.7 nM (lane 4), or 0.43 nM (lane 5) VPF/VEGF. The 3' boundary shown in (b) was determined in the same manner with 5'-labeled ligand (same lane assignments as (a)). The absence of pyrimidine nucleotide bands (due to resistance to alkaline hydrolysis of the phosphodiester bonds 3' to the 2'-aminopyrimidine nucleosides) allows sequence assignment without external markers. Arrows indicate the 5' and 3' boundaries that define the minimal ligand. Lowercase and uppercase letters indicate nucleotides in the constant and evolved sequence regions, respectively, and 2'-aminopyrimidine nucleotides are shown in italic letters.

in the unselected lane. The relative intensity of the G9 band is approximately equal in the selected and unselected lanes. These observations suggest a preference for 2'-OH adenosine at position 14 and for 2'-OMe adenosine at position 12. No preference for either 2'-OMe or 2'-OH guanosine is observed at position 9.

Band intensities were quantitated by phosphorimager analysis and expressed as a fraction of total counts (pixels) in each lane. Since the partial 2'-OMe substitution was split between four ligand pools (see Materials and methods), each unsubstituted ribopurine position occurs three times. The mean of the three unsubstituted normalized band intensity ratios for the unselected versus the selected lanes is plotted as a function of purine nucleotide position in Figure 4b. These values provide a standard against which the effect of the 2'-OMe substitution on binding can be quantitated. The curvature results from the difference in the extent of partial alkaline hydrolysis in the unselected and the selected lanes. Normalized band intensity ratios for the partially 2'-OMe-substituted positions that are significantly above or below the curve fit line for the unselected lanes compared with those for the selected lanes (Fig. 4b) reveal positions where the 2'-OMe substitution reduces (G6, A7, G10, A14) or enhances (G16) binding affinity.

Binding of minimal ligands to VPF/VEGF

We used this information to synthesize an analog of ligand NX-107 in which all but four purine nucleotides (G6, A7, G10, A14) were substituted with the 2'-OMe group. To minimize degradation by the exonucleolytic pathway, we also added short poly dT segments containing four contiguous internucleoside phosphorothioate linkages to the 5' end ([5'P] = d(TsTsTsTs), where s represents the phosphorothioate linkage) and the 3' end ([3'P] = d(TsTsTsTsT)). The addition of phosphorothioate caps does not significantly affect binding to VPF/VEGF (data not shown). The minimal 2'-OMe-substituted ligand with the phosphorothioate caps will be referred to as NX-213. Binding of NX-213 to VPF/VEGF is compared in Figure 5 to that of the 2'-OMe-unsubstituted ligand (NX-178), a ligand in which the 2'-OMe substitution pattern in purine nucleotides is inverted compared to NX-213 (NX-223), a ligand in which all purine nucleotides are 2'-OMe-substituted (NX-224) and a ligand in which all nucleotides are 2'-OMe-substituted (NX-191). The K_d values for these ligands are given in Table 1. The 2'-OMe substitution at permissive purine nucleotide positions increases the binding affinity for VPF/VEGF ≈17-fold. Conversely, the 2'-OMe substitution at purine nucleotide positions that prefer the 2'-OH group or at all positions in the ligand abrogates high-affinity binding.

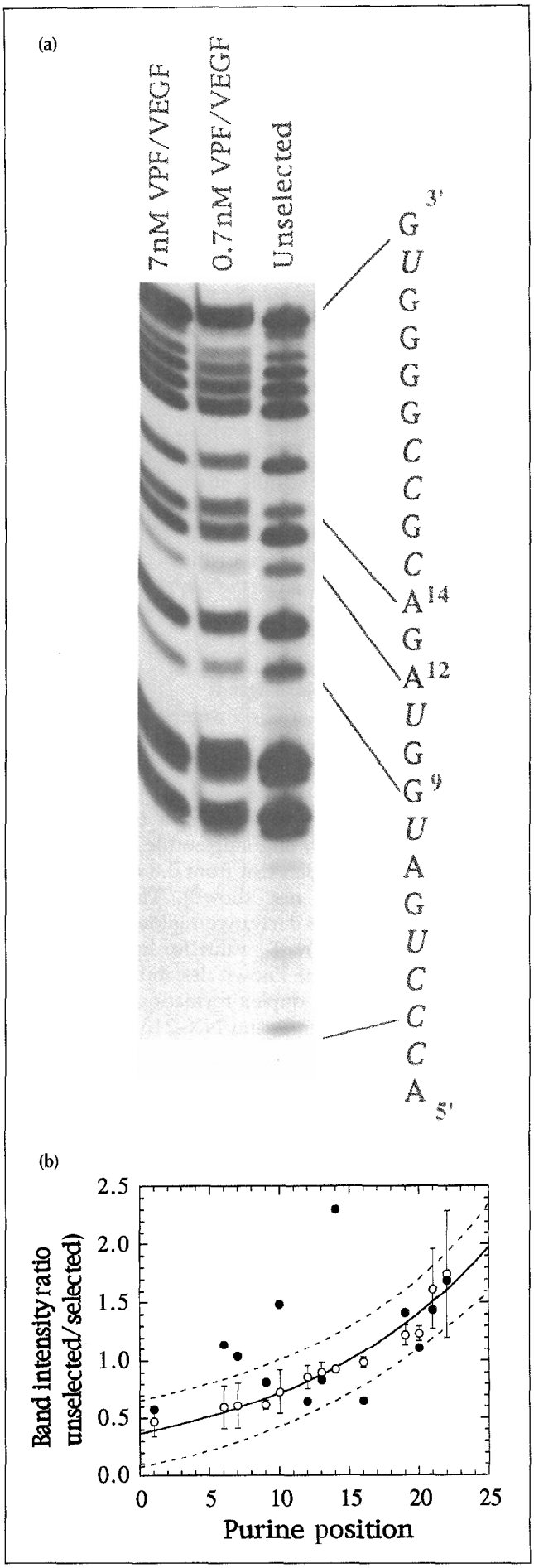

Fig. 4. 2'-O-Methylpurine nucleotide interference analysis indicates positions that can be substituted without compromising binding affinity to VPF/VEGF. **(a)** Minimal VPF/VEGF ligand NX-107 was chemically synthesized to contain a mixture of 2'-OMe and 2'-OH purine nucleotides at positions 9, 12, and 14, using a 2:1 molar ratio of 2'-OMe:2'-OH (protected as the *t*-butyldimethylsilyl ether) phosphoramidites (pool A). Other purine nucleotides are unmodified (2'-OH) and all pyrimidine nucleotides (shown in italics) are 2'-amino-modified. The unselected lane shows the partial alkaline hydrolysis pattern of the ^{32}P 5'-end-labeled ligand population prior to affinity selection resolved on a 20 % polyacrylamide denaturing gel. The phosphodiester bonds 3' to the 2'-aminopyrimidine nucleosides are essentially resistant to alkaline hydrolysis resulting in the absence of bands at those positions (see also Fig. 3). Partial 2'-OMe substitution at positions 9, 12, and 14 is reflected in fainter bands compared to those of the neighboring ribopurines. The first two lanes from the left show the partial alkaline hydrolysis pattern following affinity selection with 7 nM or 0.7 nM protein. The preference for the 2'-OMe or the 2'-OH group at the three substituted positions is deduced from the differences in the relative band intensities in the affinity-selected versus the unselected ligand pools. For example, the preference for the 2'-OH group at position 14 is deduced from the ratio of A14 to G13 band intensities, which is greater in the affinity-selected lanes than in the unselected lane. Similarly, the preference for the 2'-OMe group at position 12 is deduced from the ratio of A12 to G13 band intensities, which is lower in the affinity-selected lanes than in the unselected lane. Band intensities were quantitated by phosphorimager analysis and the data were normalized for differences between lanes and the extent of partial alkaline hydrolysis (see (b)). **(b)** Graphic representation of the normalized phosphorimager data for determination of the 2'-OMe purine nucleotide substitution pattern. The mean of the three normalized band intensity ratios (unselected/selected lanes) for the unsubstituted (exclusively 2'-OH) purine positions is shown in open circles, with standard deviations. A smooth curve is drawn through the data points to guide the eye ($y = 0.403e^{0.609x}$); the 95 % confidence intervals are shown in dashed lines. The equivalent ratio for each of the partially substituted purine nucleotide positions is shown as filled circles. Ratios for the substituted positions that are significantly above or below the curve fit line reveal positions where the 2'-OMe substitution reduces (G6, A7, G10, A14) or enhances (G16) binding affinity, respectively.

We also determined the dissociation rates for complexes of ligands NX-178 and NX-213 with VPF/VEGF at 37 °C using radiolabeled ligands and adding a large molar excess (≈500-fold) of the unlabeled ligands (Fig. 5b). For both ligands, the first-order rate equation provides an adequate fit to the data points. The dissociation rate constants obtained from these data were $5.9 \pm 0.7 \times 10^{-2}$ s^{-1} ($t_{1/2}$ = 12 s) for NX-178 and $1.4 \pm 0.6 \times 10^{-3}$ s^{-1} ($t_{1/2}$ = 8 min) for NX-213. Assuming a simple bimolecular association model, the association rate constants of $2.4 \pm 0.6 \times 10^7$ M^{-1}s^{-1} for NX-178 and $1.0 \pm 0.4 \times 10^7$ M^{-1}s^{-1} for NX-213 were calculated. The 2'-OMe substitution at permissive purine nucleotide positions therefore decreases the dissociation rate constant ≈40-fold and the association rate constant ≈2-fold.

We next tested whether the ligands bind to a biologically relevant site on the protein. Figure 5c shows that NX-213 inhibits binding of ^{125}I-labeled VPF/VEGF to the receptors expressed on human umbilical vein endothelial cells (HUVECs) in a concentration-dependent manner with an ED_{50} of ≈1 nM. The ED_{50} for the control ligand NX-191 is >1 μM.

Table 1. Dissociation constants (K_ds) and melting temperatures (T_ms) for minimal ligands derived from clone 24A.

Ligand	Structure[a]	K_d, nM[b]	T_m[c], °C
NX-178	5'-[5'P]A*CCCU*GA*U*GG*U*AGA*C*G*CC*GGGG*U*G[3'P]-3'	2.4 ± 0.5	39
NX-190	5'-[5'P]d(ACCCTGATGGTAGACGCCGGGGTG)[3'P]-3'	–	44
NX-191	5'-[5'P]A*CCCU*GA*U*GG*U*AGA*C*G*CC*GGGG*U*G[3'P]-3'	250 ± 130	73
NX-213	5'-[5'P]A*CCCU*GA*U*GG*U*AGA*C*G*CC*GGGG*U*G[3'P]-3'	0.14 ± 0.01	46
NX-223	5'-[5'P]A*CCCU*GA*U*GG*U*AGA*C*G*CC*GGGG*U*G[3'P]-3'	250 ± 100	–
NX-224	5'-[5'P]A*CCCU*GA*U*GG*U*AGA*C*G*CC*GGGG*U*G[3'P]-3'	320 ± 70	–

[a]2'-Aminopyrimidine nucleotides are designated with italic letters; 2'-OMe purine nucleotides are underlined; [5'P] represents the 5' cap, d(TsTsTsTs), where s represents the internucleoside phosphorothioate linkage, and [3'P] represents the 3' cap, d(TsTsTsTsT).
[b]K_d values were determined from the data shown in Figure 5.
[c]T_m values were determined from the data shown in Figure 8.

We examined the specificity of NX-178 and NX-213 binding by measuring their K_ds with a panel of heparin-binding proteins (Table 2). The affinity of both ligands for native VPF/VEGF is significantly higher than that for any other protein examined. Although the affinity of NX-213 for native VPF/VEGF is 17-fold greater than that of NX-178, the affinities of these two ligands for other proteins are comparable; the improvement in affinity for native VPF/VEGF is therefore coupled to the improvement in specificity.

Thermal stabilities of minimal ligands

Melting temperatures (T_ms) were determined for ligands NX-178, NX-213, NX-190 (the all-DNA equivalent of NX-213) and NX-191 from the UV absorption versus temperature profiles (Fig. 6). Thermal denaturation data were determined at three different concentrations for each oligonucleotide and shown to be concentration independent from 0.8 to 40 μg ml^{-1} oligonucleotide (data not shown). The T_m values obtained from the first derivative replots (Fig. 6b) are listed in Table 1. The low T_m value for ligand NX-178 is expected based on the known destabilizing effect of the 2'-amino group on duplex formation [37–39]. The 2'-OMe substitutions in ligand NX-213, on the other hand, lead to a significant (≈7 °C) increase in the thermal stability. The stabilizing effect of the 2'-OMe substitutions on RNA:RNA or RNA:DNA duplex formation has been observed previously [40,41] and is further evident in the large increase in the T_m observed in the fully 2'-OMe-substituted molecule, NX-191. The thermal transitions observed here correspond to the helix-to-coil transitions of the monomeric (hairpin) species of oligonucleotides. With NX-213 and NX-191, we have not detected significant intermolecular duplex formation on non-denaturing polyacrylamide gels; only the monomeric species were observed as single bands at nucleic acid concentrations up to 400 μM (data not shown).

Secondary structure of NX-213

The predicted secondary structure of NX-213 based on base-pairing covariation (Fig. 1), consensus base-pairing analysis (Fig. 2), and preliminary 1D and 2D ^1H NMR data on NX-213 and other analogs (not shown) is a bulged hairpin (Fig. 7). The NMR results suggest that a stable four-base-pair stem is formed involving three G–*C* base pairs and an A–*U* base pair and that this stem is disrupted at or after *U*5/G19. Interestingly, a longer stem with an additional *U*–G and G–*C* base pair does not appear to form, or may form only transiently. This less stable stem might be a result of the 2'-amino modifications, which are known to destabilize helical conformations [37–39].

Table 2. Binding affinities (K_d values) and specificity indices ($K_d^{Protein}/K_d^{VPF/VEGF}$) of NX-178 and NX-213 for native VPF/VEGF, reduced VPF/VEGF, platelet-derived growth factor AB (PDGF-AB), basic fibroblast growth factor (bFGF), antithrombin III (ATIII) and thrombin[a].

	NX-178		NX-213	
Protein	K_d, nM	$K_d^{Protein}/K_d^{VPF/VEGF}$[b]	K_d, nM	$K_d^{Protein}/K_d^{VPF/VEGF}$[b]
VPF/VEGF	2.4 ± 0.5	(1.0)	0.14 ± 0.01	(1.0)
Red. VPF/VEGF[c]	308 ± 89	1.3 x 102	280 ± 76	2.0 x 103
PDGF-AB	75 ± 21	3.1 x 101	91 ± 30	6.5 x 102
bFGF	322 ± 44	1.3 x 102	286 ± 23	2.0 x 103
ATIII	1920 ± 92	8.0 x 102	6270 ± 559	4.5 x 104
Thrombin	3010 ± 259	1.3 x 103	3060 ± 106	2.2 x 104

[a]All K_d values were determined by nitrocellulose filter binding.
[b]Specificity index is defined as the ratio of dissociation constants for any protein to native VPF/VEGF.
[c]VPF/VEGF was reduced by incubation in 10 mM dithiothreitol for 5 min at room temperature.

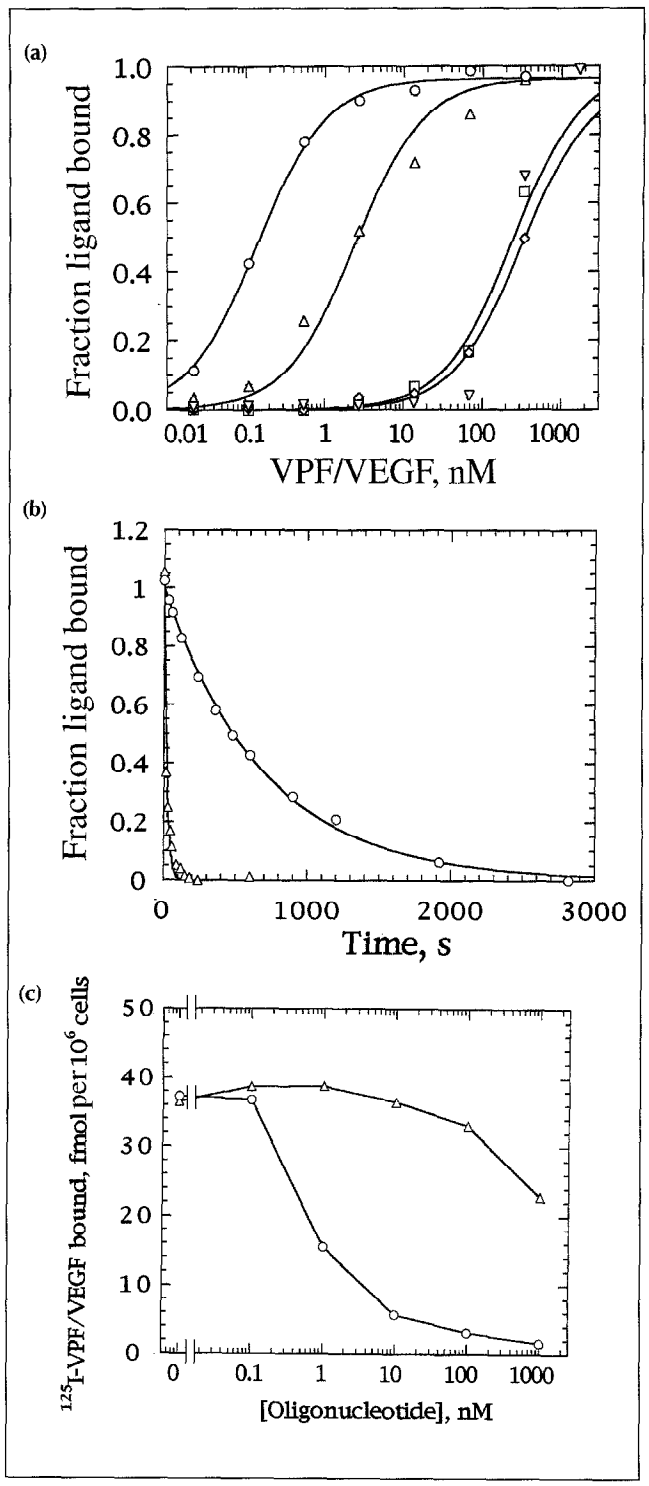

Fig. 5. Modifications at the 2' positions of SELEX-derived ligands alter their affinity for VPF/VEGF. **(a)** Binding of oligonucleotide ligands to VPF/VEGF. The fraction of ^{32}P 5'-end-labeled oligonucleotide bound to varying concentrations of VPF/VEGF was determined by the nitrocellulose filter binding method. Oligonucleotides tested were ligand NX-213 (○), NX-178 (△), NX-223 (□), NX-224 (◇) and NX-191 (▽). Oligonucleotide concentrations in these experiments were <50 pM. The lines represent the least squares fit of the data points to the binding equation $q=f[P]/\{[P]+K_d\}$ where q is the fraction of protein-bound RNA, [P] is the free protein concentration and f is the efficiency of retention of the VPF/VEGF–RNA complexes on nitrocellulose filters. For ligands NX-223 and NX-224, background binding to nitrocellulose in the absence of protein amounting to 5 and 14 %, respectively, of the maximal signal was observed and was subtracted from all values. Each data point represents the average of two determinations. Binding reactions were done at 37 °C in PBS containing 0.01 % HSA. **(b)** 2'-OMe substitution at permissive purine nucleotide positions decreases the dissociation rate of the ligand–VPF/VEGF complex. Dissociation of ligands NX-178 (△) and NX-213 (○) from VPF/VEGF under pseudo first-order conditions is shown. For each ligand, the fraction of ^{32}P 5'-end-labeled ligand bound to VPF/VEGF was measured at the indicated time points following the addition of 500-fold excess of the unlabeled competitor ligand. The dissociation rate constant (k_{off}) was determined by fitting the data points to the first-order rate equation $[(A-A_\infty)/(A_0-A_\infty)] = \exp(-k_{off}t)$, where A, A_0 and A_∞ represent the normalized fractions of RNA bound to VPF/VEGF at any time (t), t = 0 and t = ∞, respectively. The experiment was performed at 37 °C in PBS containing 0.01 % HSA. **(c)** Oligonucleotide ligand NX-213 blocks binding of ^{125}I-VPF/VEGF to cell-surface receptors expressed on human umbilical vein endothelial cells (HUVECs). Confluent cultures of HUVECs were incubated with ^{125}I-VPF/VEGF (10 ng ml^{-1}) and varying amounts of NX-213 (○) or NX-191 (△) for 2 h at 4 °C. The amount of cell-associated radioactivity was determined as described in the Materials and methods section. Data points represent averages of two determinations.

Nuclease resistance of modified nucleic acid ligands

To be effective therapeutics, nucleic acid ligands must resist rapid degradation by nucleases. To test the effect of the addition of phosphorothioate caps and the 2'-OMe substitution, we examined the stability of ligands NX-107, NX-178 and NX-213 in undiluted rat urine over a period of 21 h (Fig. 8). In general, urine has a greater capacity to degrade nucleic acid ligands compared to serum or plasma. The considerable improvement in stability of NX-178 ($t_{1/2}$ = 17 ± 2 h) compared to NX-107 ($t_{1/2}$ = 1.4 ± 0.1 h) attests to the utility of protecting the ligands against degradation by exonucleases. The 2'-OMe substitution at 10 out of 14 purine nucleotides in NX-213 imparts an additional increase in ligand stability ($t_{1/2}$ = 131 ± 4 h). Similar results have been obtained in other biological fluids and tissues such as liver, kidney, brain and spleen (L. Green and N. Janjić, unpublished observations) as well as in preliminary pharmacokinetic studies.

Discussion

Reproducible identification of VPF/VEGF ligands

Amplifiable nuclease-resistant oligonucleotide libraries are becoming increasingly important in the discovery of nucleic acid-based drug candidates. This is largely due to the reduction in the number of modifications required to convert lead SELEX-derived compounds with desirable *in vitro* properties into drug candidates with favorable bioavailabilities. We have recently demonstrated that the ability of the SELEX process to reproducibly identify rare nucleic acid ligands that bind to bFGF with high affinity is not compromised by the use of nuclease-resistant (2'-aminopyrimidine RNA) libraries. In the SELEX experiments reported here, we observed the emergence of a common consensus sequence motif that imparts high-affinity binding to VPF/VEGF. It is worth noting that in the sequence set shown in Figure 1, the 17-nucleotide

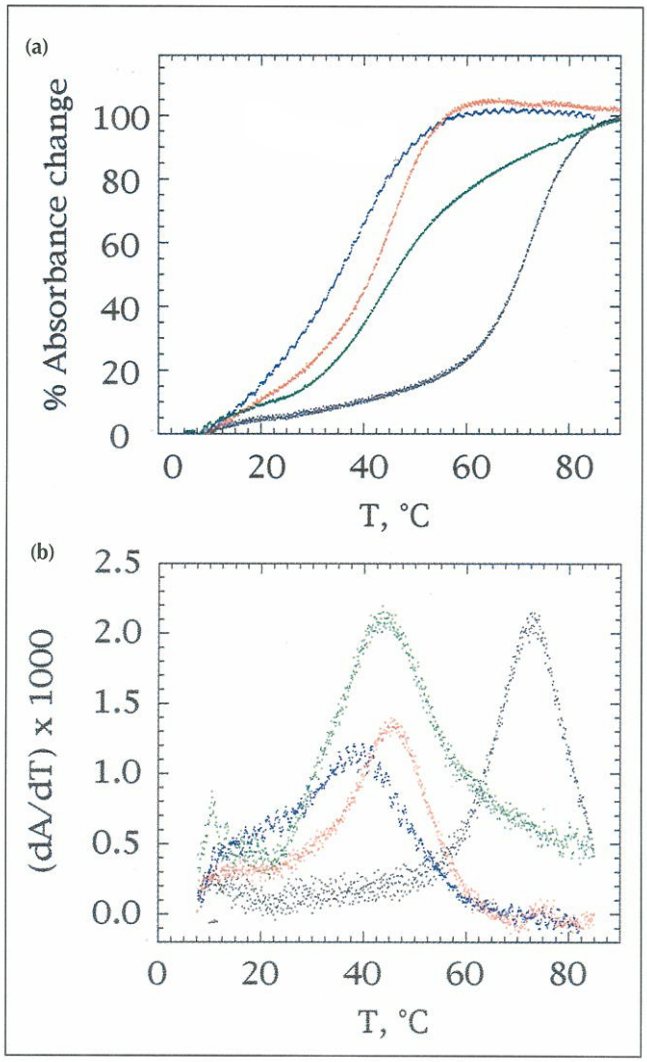

Fig. 6. Modifications at the 2' positions of SELEX-derived ligands for VPF/VEGF alter their thermal stability. Thermal denaturation profiles of VPF/VEGF oligonucleotide ligands. **(a)** The change in absorbance at 260 nm was measured as a function of temperature for ligands NX-178 (blue), NX-213 (red), NX-190 (green) and NX-191 (black). **(b)** The first derivatives of the data shown in (a).

consensus sequence, 5'-*CU*GA*U*GG*U*AGACG*CC*GG-3', is almost completely conserved, with only three positions deviating from the consensus in one out of six ligands in the family. The frequency of occurrence of the consensus secondary structure motif, 5'-NNN*CU*GA*U*GG*U*AGACG*CC*GGN'N'N'-3' (underlined arrows indicate base pairing), in a region of 30 (SELEX A) or 50 (SELEX B) contiguous randomized positions is estimated from its information content [42] to be 2.5×10^{-11} or 8.6×10^{-11}, respectively. In the initial random libraries A and B, which contained about 6×10^{14} molecules each, this motif is expected to occur 1.5×10^{4} and 5.2×10^{4} times, respectively. While the information content of this motif is not small, we have in previous SELEX experiments isolated ligands that occur much less frequently [31,32,43]. Ligands with this secondary structure motif, given their information content, represent a surprisingly small fraction (6/43 or 14 %) of the VPF/VEGF-binding sequences isolated from the affinity-enriched pool. This indicates that additional rounds of selection/amplification may result in the emergence of ligands with even higher affinities for VPF/VEGF that were more sparsely represented in the initial random pool.

Secondary structure analysis

The detection of consensus primary structure, either by inspection or with the aid of multiple sequence alignment algorithms, is generally straightforward for families composed of relatively short sequences in which a highly conserved sequence region is shared by all members (Fig. 1). As a consequence of their functional relatedness, all ligands in a family are expected to have broadly similar secondary and tertiary structures. The consensus secondary structure identification, however, is usually considerably more difficult. The difficulty largely comes from the fact that several possible secondary structures with comparable predicted free energies of folding exist for many individual sequences. Nevertheless, the functionally relevant secondary structure in a sequence set should be accessible to all ligands. The overlayed dot-matrix representation of base pairing was developed as a way of simultaneously viewing all possible base pairings for all ligands in a family in a manner that enhances the common motif by signal amplification [34]. The multitude of alternative secondary structures is apparent in the unfiltered matrix pattern (upper-right triangle in Fig. 2). Note that this matrix pattern is characterized not only by strong overlap at certain positions but also by a striking lack of all possible secondary structures in other regions. The restricted spectrum of conformations undoubtedly contributes to the rigidity of nucleic acid ligands, which is expected to have a favorable entropic effect on binding. With proper sequence alignment, the consensus secondary structure clearly emerges after weaker secondary structures are filtered out (lower left triangle, Fig. 2).

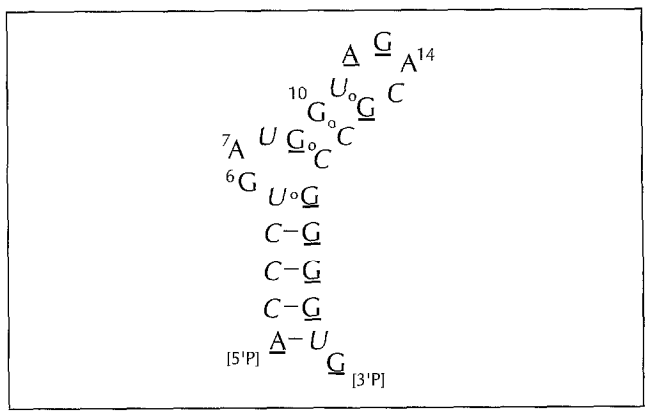

Fig. 7. The proposed secondary structure of NX-213. Base pairs in the more flexible region of the molecule are indicated by open circles. 2'-OMe purine nucleotides are underlined and the remaining ribopurines are numbered. The 2'-aminopyrimidine nucleotides are designated with italic letters. This secondary structure is consistent with the consensus secondary structure analysis (Figs 1 and 2), the base-pairing covariation analysis and the ^{1}H-NMR data.

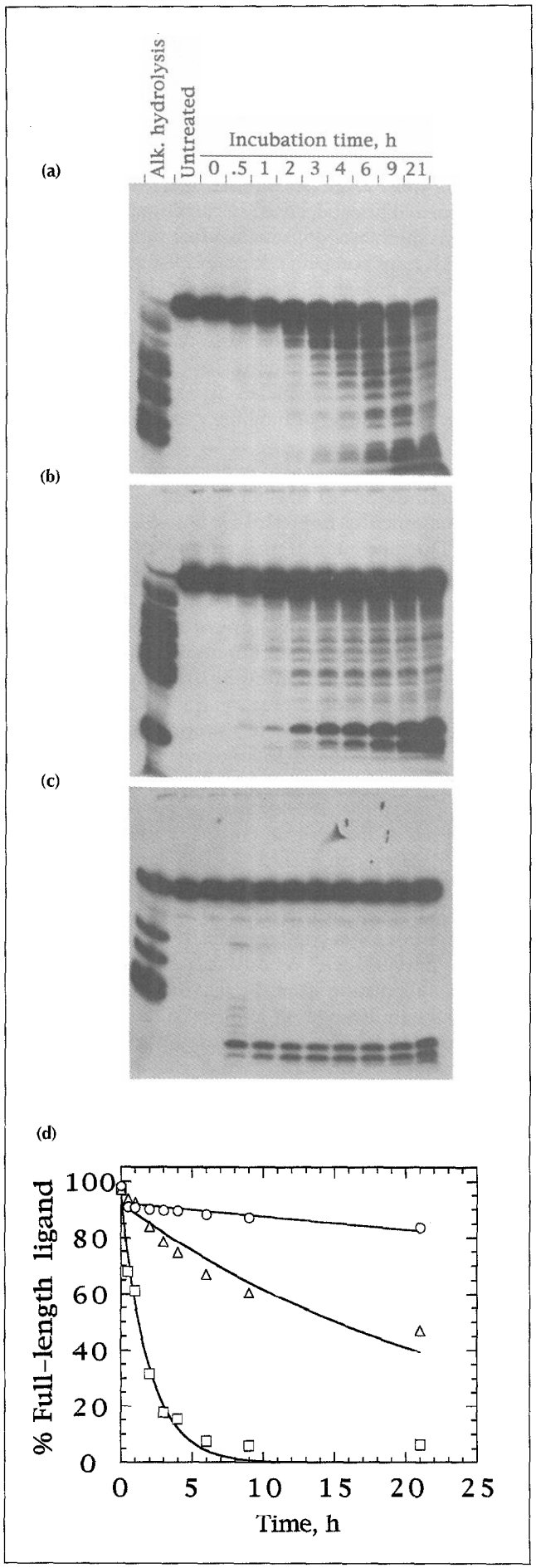

Fig. 8. Modification of ligands for VPF/VEGF alters their nuclease sensitivity. The stability of ligands NX-107, NX-178 and NX-213 in rat urine is shown. Aliquots from the incubation mixtures of 5'-end-labeled **(a)** NX-107, **(b)** NX-178 and **(c)** NX-213 in sterile rat urine were removed at indicated time points and resolved on 20 % polyacrylamide gels containing 7 M urea. **(d)** The percentage of the full-length NX-107 (❑), NX-178 (Δ) and NX-213 (O) remaining at each time point was determined by phosphorimager analysis. Solid lines represent the least-squares fit of the data points to the first-order rate equation.

Post-SELEX modifications: increased nuclease resistance and affinity maturation

The 2'-OMe interference experiment was initiated primarily to further increase the *in vivo* stability of the lead ligand. Indeed, the partially 2'-OMe-substituted ligand NX-213 is considerably more nuclease-resistant than its unsubstituted analog (NX-178). All but four of the purine nucleotides in the ligand tolerate the 2'-OMe substitution. In an analogous interference experiment with a SELEX-derived RNA ligand to HIV RT, Green *et al.* [44] have recently shown that the 2'-OMe group could be substituted at all but two positions. These observations suggest that this and other similar modification interference analyses are generally applicable methods of stabilizing SELEX ligands against nuclease degradation.

Although the permissive 2'-OMe substitution pattern in ligand NX-213 was determined on the basis of affinity selections and at least one purine nucleotide (G16) exhibited a considerable preference for the 2'-OMe group (Fig. 5), the increase in binding affinity of 17-fold compared to the unsubstituted compound was not anticipated. The origin of the 2'-OMe substitution-related affinity improvement is at present not clear. The design of the interference experiment has allowed us to examine the effect of 2'-OMe substitution on binding at multiple positions simultaneously. However, since the quantitative relationship between the 2'-OMe preference index (Fig. 5) and the K_d values of singly-substituted ligands has not yet been defined, we do not know whether the observed improvement in binding of NX-213 is due to the 2'-OMe substitution at a few key positions (e.g. G16) or to the multiplicative effect of substituting most of the purine nucleotides in the molecule. Global substitution-related changes such as the increased hydrophobic character or the greater thermal stability of NX-213 compared to NX-178 could be responsible for part of the observed affinity improvement.

All of the affinity improvement appears to be the result of the decrease in the dissociation rate constant of NX-213 compared to that of NX-178, since the calculated association rate constant of NX-178 is actually about two-fold greater than that of NX-213. With values of 1–3 x 10^7 $M^{-1}s^{-1}$, the association rate constants of these ligands are large enough to be close to the diffusion-controlled limit [45]; a significant improvement in binding affinity through a large increase in the association rate is therefore improbable. It is worth noting that association rates of this magnitude are not unusual for the binding of

nucleic acid ligands to their target proteins; for example, the value of 1 x 10^8 $M^{-1}s^{-1}$ was obtained for the binding of HIV Tat peptide fragment (Trf-38) to its RNA target sequence (ΔTAR) [46] and 1–2 x 10^8 $M^{-1}s^{-1}$ for the binding of tRNA synthetases to their cognate tRNAs [45]. For the ligands described here, further improvement in binding to VPF/VEGF is more likely to be achieved through an additional decrease in the dissociation rate. To function as inhibitors of growth-factor signaling, nucleic acid ligands must compete with the cell-surface receptors for binding to growth factors. Since the dissociation rates of many growth factors (including VPF/VEGF) from their high affinity receptors are typically very slow [47–49], the kinetic stability of the oligonucleotide–growth factor complexes is expected to be an important determinant of inhibitory effectiveness.

The 2'-OMe interference experiment demonstrates that the affinity of SELEX-derived nucleic acid ligands can be substantially improved by post-SELEX modifications. The notion that the affinity of nucleic acid ligands can be increased by modifying the original ligand is not new. For example, binding affinity of the RNA replicase translational operator to the bacteriophage R17 coat protein was improved ≈10-fold upon a phosphodiester to phosphorothioate (the R_p isomer) substitution at a single position [50] and ≈100-fold upon a uridine to cytidine substitution, also at a single position [51]. The need to improve the affinity of a ligand derived from SELEX will be dictated by the affinity of the initial lead compounds as well as by the intended use of the ligands. For many uses, affinities in the low nanomolar range, which are typical for SELEX-derived ligands, will be sufficient. In cases where it is needed, further affinity enhancement can be achieved through secondary SELEX experiments or through post-SELEX modifications, using in both instances information from the first SELEX experiment as a lead. A similar type of affinity-enhancement strategy is used during an immune response to antigens in which antibodies, after the initial gene recombination step that generates binding-site diversity, undergo somatic mutation of their variable region genes followed by antigen-dependent selection, in a process known as affinity maturation [52]. In the example presented here, a substantial improvement in affinity for VPF/VEGF was achieved with a single type of functional group, substituting only at the 2' position. More efficient post-SELEX modulation of nucleic acid ligand properties is expected with a larger repertoire of functional groups (including other combinatorial libraries) and substitutions over a range of positions in the ligand. In a sense, a SELEX-derived nucleic acid ligand can be thought of as a precisely constructed scaffold that can be subsequently decorated with a wide variety of function-modulating chemical moieties.

As a highly nuclease-resistant modified oligonucleotide, NX-213 is a prototype of the next generation of SELEX ligands. The effect of binding of NX-213 on the functional properties of VPF/VEGF *in vitro* and *in vivo* is currently being examined.

Significance

New blood vessel growth (angiogenesis) is increasingly recognized as an important driving force behind many proliferative disorders. As the molecular basis of angiogenesis becomes elucidated, the opportunity arises to develop pharmacologic agents that interfere with the critical events along the stimulus-to-response pathway. VPF/VEGF appears to be one of the key positive regulators of angiogenesis; inhibitors of VPF/VEGF function may be valuable in the therapy of psoriasis, rheumatoid arthritis, retinopathies and certain cancers.

Screening of random nucleic acid libraries with the SELEX combinatorial chemistry process has recently emerged as a powerful tool for identifying molecules with useful functional properties. For identification of nucleic acid-based drug candidates, the use of nuclease-resistant libraries is highly desirable. In this report, we have used the SELEX process to identify nuclease-resistant 2'-aminopyrimidine RNA ligands that bind to VPF/VEGF with high affinity. We have also demonstrated that the affinity, specificity and nuclease resistance can be further improved with post-SELEX modifications. With continuing improvements in solid-phase oligonucleotide synthesis, these relatively short oligonucleotides can now be synthesized in sufficient amounts to allow examination of their potential as diagnostic, imaging and therapeutic agents.

Materials and methods

Materials

Recombinant human VPF/VEGF (165-amino-acid isoform) was purchased from R&D Systems (Minneapolis, MN) as a lyophylized powder free from carrier protein. Recombinant human basic fibroblast growth factor, and platelet-derived growth factor (AB heterodimer) were also from R&D Systems. Human antithrombin III and thrombin were purchased from Enzyme Research Laboratories (South Bend, IN). 2'-Amino-2'-deoxypyrimidine 5'-triphosphates were prepared in our laboratories as described [53]. The 2'-aminopyrimidine nucleoside phosphoramidites for solid-phase synthesis were prepared by standard methods [54,55] and the 2'-amino group was protected as the trifluoroacetyl derivative [56]. Synthetic oligonucleotides were prepared on an Applied Biosystems Model 394 oligonucleotide synthesizer according to the manufacturer's protocols.

The SELEX process

Iterative rounds of selection/amplification were performed as described [31,32]. Briefly, 2'-aminopyrimidine RNA containing a randomized region of 30 or 50 nucleotides was prepared by *in vitro* transcription from synthetic DNA templates [57] as described [31]. In SELEX experiment A, the starting RNA containing 30 randomized positions (5'-gggagacaagaauaacgcu-

caa[30N]*uucgacaggaggcucacaacaggc*-3' (lower-case letters indicate the constant regions, italics to indicate 2'-aminopyrimidine nucleotides, throughout this paper), was used with the corresponding primers (5'-d(taatacgactcactatagggagacaagaataacgctcaa)-3' and 5'-d(gcctgttgtgagcctcctgtcgaa)-3'). In SELEX experiment B, the starting RNA containing 50 randomized positions (5'-gggaggacgaugcgg[50N]cagacgacucgcccga-3') was used with its corresponding primers (5'-d(taatacgactcactatagggaggacgatgcgg)-3' and 5'-d(tcgggcgagtcgtctg)-3'). After *in vitro* transcription the RNA was purified on 8 % polyacrylamide gels containing 7 M urea, eluted from the gel by the crush and soak method, alcohol precipitated and resuspended in phosphate buffered saline (PBS: 10.1 mM Na_2HPO4, 1.8 mM KH_2PO_4, 137 mM NaCl and 2.7 mM KCl, pH 7.4). Prior to incubation with VPF/VEGF, the RNA was heated at 90 °C for 2 min and cooled on ice. Stock solutions of VPF/VEGF were prepared by resuspending the lyophilized protein in PBS at concentrations of 5–10 μM. VPF/VEGF stock solution concentrations were determined for each lot from the absorbance at 280 nm and the extinction coefficient of 1.3 x 10^4 $M^{-1}cm^{-1}$ for VPF/VEGF dimer. Affinity selections were done by incubating VPF/VEGF with RNA for at least 15 min at 37 °C in PBS containing 0.01 % human serum albumin. Partitioning of free RNA from protein-bound RNA was done by nitrocellulose filtration [32]. Protein-bound RNA was extracted from the nitrocellulose filters by soaking the minced filters in a mixture of phenol (400 μl, pH 7) and 7 M urea (200 μl) in 1.5 ml microfuge tubes for 30 min at room temperature, separating the phases by centrifugation and washing the aqueous layer with phenol and chloroform. The RNA was precipitated by adding one-tenth volume of 3 M sodium acetate (adjusted to pH 7 with acetic acid) and two volumes of 1:1 mixture of ethanol and isopropanol. Reverse transcription and PCR amplification were done as described [31]. Cloning and sequencing of the affinity-enriched pools was performed using established protocols [33].

2'-O-Methyl (2'-OMe) purine nucleotide interference analysis

Partially 2'-OMe-substituted oligonucleotide ligand pools were synthesized by the solid-phase phosphoramidite method using a 2:1 (mol:mol) mixture of 2'-OMe:2'-OH purine nucleoside phosphoramidites at specified positions. Four oligonucleotide pools were prepared in which 3–4 defined purine nucleotide positions contained either a 2'-OMe or a 2'-OH group; the remainder are unmodified ribopurines: pool A, 5'-A*CCCU*-GA*UG*^{9}*GUA*^{12}GA^{14}*CGCCGGGGUG*-3' (positions containing a mixture of 2'-OMe and 2'-OH purine nucleotides are numbered); pool B, 5'-A^{1}*CCCUGA*^{7}*UGGUAGACGCC*-G^{19}GG^{21}*GUG*-3'; pool C, 5'-A*CCCUG*^{6}*AUGGUAGACG*-*CCGG*^{20}*GGUG*^{24}-3'; and pool D, 5'-A*CCCUGAUGG*^{10}*UA*-G^{13}*ACG*^{16}*CCGGGGUG*-3'. The four pools were 5' end-labeled with [γ-^{32}P]ATP and T4 polynucleotide kinase and purified by gel electrophoresis to ensure size homogeneity.

The pools were then incubated separately with 7 and 0.7 nM VPF/VEGF in PBS containing 0.01 % HSA for 15 min at 37 °C and the protein-bound ligands were selected by nitrocellulose filter partitioning as described above. The affinity-selected and the unselected pools were subjected to partial alkaline hydrolysis (50 mM sodium carbonate buffer, pH 9.0, 90 °C for 10–20 min) and the hydrolytic fragments were resolved on 20 % polyacrylamide denaturing gels. Dried gels were exposed to Fuji type BAS-IIIs imaging plates and the band intensities were quantitated on a Fuji Model BAS1000 Bio-imaging Analyzer. The data were normalized to the sum of the band intensities for each lane, and the ratio of the selected to the unselected normalized values was determined for each position.

Apparent equilibrium dissociation constant and dissociation rate constant determinations

The binding of oligonucleotide ligands at low concentrations to varying concentrations of VPF/VEGF and other proteins was measured using the nitrocellulose filter binding assay as described [32,43]. Oligonucleotides for all binding experiments were purified by denaturing polyacrylamide gel electrophoresis and subjected to a thermal denaturation/renaturation cycle as described above in binding buffer at high dilution (≈1 nM) prior to incubation with the protein [32,43]. Before partitioning on nitrocellulose filters, the binding mixtures were typically incubated at 37 °C for 15 min. Some ligands were affinity purified on a small scale by nitrocellulose filtration prior to the binding experiments to remove the low affinity binding fractions [31]. The dissociation rate constant for ligands NX-178 and NX-213 were determined under pseudo first-order conditions by measuring the amount of ^{32}P 5'-end-labeled ligands (≈50 pM) bound to VPF/VEGF (17 nM) as a function of time following the addition of ≈500-fold excess of the unlabeled ligands, using nitrocellulose filter binding as the partitioning method.

Receptor binding

VPF/VEGF was radioiodinated by the Iodogen method [47] to a specific activity of 1–6 x 10^4 cpm ng^{-1}. Human umbilical vein endothelial cells (HUVECs, population doubling 5) were plated in 24-well plates at a density of 1–2 x 10^5 cells per well in EGM (Clonetics, San Diego, CA). At confluence, the cells were incubated for 2 h at 4 °C in PBS containing 0.1% human serum albumin, 10 ng ml^{-1} ^{125}I-labeled VPF/VEGF and varying concentrations of the oligonucleotide ligands. At the end of the 2 h incubation period, the supernatant was aspirated and the wells were washed two times with cold PBS. HUVECs were then lysed with 1 % triton X-100 and the amount of cell-associated ^{125}I-VPF/VEGF was determined by gamma counting.

Melting temperature (T_m) measurements

Melting profiles for all oligonucleotides were obtained on a Cary Model 1E spectrophotometer. Oligonucleotides (0.8–40 μg ml^{-1}) were heated to 95 °C in PBS and cooled to room temperature prior to the melting profile determination. Melting profiles were generated by recording the absorbance at 260 nm while the sample was heated at the rate of 1 °C min^{-1} from 5–95 °C. The first derivative of the data points was calculated using the plotting program KaleidaGraph (Synergy Software, Reading, PA). The first derivative values were smoothed using a 55-point smoothing function by averaging each point with 27 data points on each side. The peak of the smoothed first derivative curves was used to estimate the T_m values.

NMR spectroscopy

NMR experiments were performed on a 500 MHz Varian VXR-S spectrometer. The oligonucleotides were dialyzed with a Centricon 3 microconcentrator (Amicon, Beverly, MA) into the 10 mM sodium phosphate buffer (pH 7.4), 10 mM sodium chloride, lyophilized and dissolved in 90 % H_2O/10 % D_2O. The spectra were collected at 5 °C with a jump and return sequence for solvent suppression [58] and with maximal excitation at the imino protons (12 ppm).

Determination of ligand stability in rat urine

Ligands NX-107, NX-178, NX-213 were 5' end-labeled with [γ-^{32}P]ATP and polynucleotide kinase and incubated at the concentration of 2 nM in sterile rat urine at 37 °C. The reactions were terminated at specified time points by the addition of 87 % aqueous formamide solution containing 25 mM EDTA and 0.02 % bromophenol blue, immediately frozen in liquid nitrogen and stored at −70 °C. Undegraded (full-length) ligands were separated from the degradation products by electrophoresis in 20 % polyacrylamide gels containing 7 M urea. The fraction of the undegraded material at each time point was quantitated by phosphorimager analysis as described above.

Acknowledgements: We are indebted to Jeff Davis for his role in developing the user-friendly Consensus Matrix software. We thank Wolfgang A. Pieken and our oligonucleotide synthesis group for providing the modified nucleic acid ligands and our statistician Julie Morris for her help with data analysis. We also thank Vanessa Appleby, Barry Polisky, Edward Brody and Larry Gold for critical reading of the paper.

References

1. Folkman, J. (1971). Tumor angiogenesis: therapeutic implications. *New Engl. J. Med.* **285**, 1182–1186.
2. Folkman, J. (1995). Angiogenesis in cancer, vascular and other diesease. *Nat. Med.* **1**, 27–31.
3. Underwood, J.C. & Carr, I. (1972). The ultrastructure and permeability characteristics of the blood vessels of a transplantable rat sarcoma. *J. Pathol.* **107**, 157–166.
4. Dvorak, H.F., *et al.*, & Giovinco, P. (1979). Induction of fibrin-gel investment: an early event in line 10 hepatocarcinoma growth mediated by tumor-secreted products. *J. Immunol.* **122**, 166–174.
5. Senger, D.R., Galli, S.J., Dvorak, A.M., Peruzzi, C.A., Harvey, V.S. & Dvorak, H.F. (1983). Tumor cells secrete a vascular permeability factor that promotes accumulation of ascites fluid. *Science* **219**, 983–985.
6. Senger, D.R., Peruzzi, C.A., Feder, J. & Dvorak, H.F. (1986). A highly conserved vascular permeability factor secreted by a variety of human and rodent tumor cell lines. *Cancer Res.* **46**, 5629–5632.
7. Connoly, D. T., *et al.*, & Feder, J. (1989). Human vascular permeability factor. Isolation from U937 cells. *J. Biol. Chem.* **264**, 20017–20024.
8. Ferrara, N. & Henzel, W.J. (1989). Pituitary follicular cells secrete a novel heparin-binding growth factor specific for vascular endothelial cells. *Biochem. Biophys. Res. Commun.* **161**, 851–858.
9. Gospodarowicz, D., Abraham, J.A. & Schilling, J. (1989). Isolation and characterization of a vascular endothelial cell mitogen produced by pituitary-derived folliculo stellate cells. *Proc. Natl. Acad. Sci. USA* **86**, 7311–7315.
10. Conn, G., Soderman, D.D., Schaeffer, M.-T., Wile, M., Hatcher, V.B. & Thomas, K.A. (1990). Purification of a glycoprotein vascular endothelial cell mitogen from a rat glioma-derived cell line (GS-9L). *Proc. Natl. Acad. Sci. USA* **87**, 1323–1327.
11. Leung, D.W., Cachianes, G., Kuang, W.-J., & Goeddel, D.V. (1989). Vascular endothelial growth factor is a secreted angiogenic mitogen. *Science* **246**, 1306–1309.
12. Keck, P.J., *et al.*, & Connolly, D.T. (1989). Vascular permeability factor, an endothelial cell mitogen related to platelet-derived growth factor. *Science* **246**, 1309–1312.
13. Houck, K.A., Ferrara, N., Winer, J., Cachianes, G., Li, B. & Leung, D.W. (1991). The vascular endothelial growth factor family: identification of a fourth species and characterization of alternative splicing of RNA. *Mol. Endocrinol.* **5**, 1806–1814.
14. Tischer, E., *et al.*, & Abraham, J.A. (1991). The human gene for vascular endothelial growth factor. Multiple protein forms are encoded through alternative exon splicing. *J. Biol. Chem.* **266**, 11947–11954.
15. de Vries, C., Escobendo, J.A., Ueno, H., Houck, K., Ferrara, N. & Williams, L.T. (1992). The fms-like tyrosine kinase, a receptor for vascular endothelial growth factor. *Science* **255**, 989–991.
16. Terman, B.I., Carrion, M.E., Kovacs, E., Rasmussen, B.A., Eddy, R.L. & Shows, T.B. (1991). Identification of a new endothelial cell growth factor receptor tyrosine kinase. *Oncogene* **6**, 519–524.
17. Millauer, B., *et al.*, & Ullrich, A. (1993). High affinity vascular endothelial growth factor binding and developmental expression suggest Flk-1 as a major regulator of vasculogenesis and angiogenesis. *Cell* **72**, 835–846.
18. Myoken, Y. Kayada, Y., Okamoto, T., Kan, M., Sato, G.H. & Sato, J.D. (1991). Vascular endothelial growth factor (VEGF) produced by A-431 human epidermoid carcinoma cells and identification of VEGF binding sites. *Proc. Natl. Acad. Sci. USA* **88**, 5819–5823.
19. Kim, K.J., *et al.*, & Ferrara, N. (1993). Inhibition of vascular endothelial growth factor-induced angiogenesis suppresses tumour growth *in vivo*. *Nature* **362**, 841–844.
20. Shweiki, D., Itin, A., Soffer, D. & Keshet, E. (1992). Vascular endothelial growth factor induced by hypoxia may mediate hypoxia-initiated angiogenesis. *Nature* **359**, 843–845.
21. Plate, K.H., Breier, G., Weich, H. A. & Risau, W. (1992). Vascular endothelial growth factor is a potential tumor angiogenesis factor in human gliomas *in vivo*. *Nature* **359**, 845–848.
22. Weindel, K., Marme, D. & Weich, H. A. (1992). AIDS-associated Kaposi's sarcoma cells in culture express vascular endothelial growth factor. *Biochem. Biophys. Res. Commun.* **183**, 1167–1174.
23. Senger, D.R., *et al.*, & Dvorak, H.F. (1993). Vascular permeability factor (VPF, VEGF) in tumor biology. *Cancer Metast. Rev.* **12**, 303–324.
24. Dvorak, H.F., *et al.*, & Senger, D.R. (1991). Distribution of vascular permeability factor (vascular endothelial growth factor) in tumors: concentration in tumor blood vessels. *J. Exp. Med.* **174**, 1275–1278.
25. Millauer, B., Shawver, L.K., Plate, K.H., Risau, W. & Ullrich, A. (1994). Glioblastoma growth inhibited *in vivo* by a dominant-negative Flk-1 mutant. *Nature* **367**, 576–579.
26. Kondo, S., Asano, M., Matsuo, K., Ohmori, I. & Suzuki, H. (1994). Vascular endothelial growth factor/vascular permeability factor is detectable in sera of tumor-bearing mice and cancer patients. *Biochim. Biophys. Acta* **1221**, 211–214.
27. Gold, L. (1995). Oligonucleotides as research, diagnostic, and therapeutic agents. *J. Biol. Chem.* **270**, 13581–13584.
28. Gold, L., Polisky, B., Uhlenbeck, O. C. & Yarus, M. (1995). Diversity of oligonucleotide functions. *Annu. Rev. Biochem.* **64**, 763–797.
29. Lin, Y., Qiu, Q., Gill, S.C. & Jayasena, S. (1994). Modified RNA sequence pools for *in vitro* selection. *Nucleic Acids Res.* **22**, 5229–5234.
30. Latham, J.A., Johnson, R. & Toole, J.J. (1994). The application of a modified nucleotide in aptamer selection: novel thrombin aptamers containing 5-(1-pentynyl)-2'-deoxyuridine. *Nucleic Acids Res.* **22**, 2817–2822.
31. Jellinek, D., *et al.*, & Janjić, N. (1995). Potent 2'-amino-2'-deoxypyrimidine RNA inhibitors of basic fibroblast growth factor. *Biochemistry* **34**, 11303–11372.
32. Jellinek, D., Green, L. S., Bell, C. & Janjić, N. (1994). Inhibition of receptor binding by high-affinity RNA ligands to vascular endothelial growth factor. *Biochemistry* **33**, 10450–10456.
33. Schneider, D., Tuerk, C. & Gold, L. (1992). The selection of high affinity RNA ligands to the bacteriophage R17 coat protein. *J. Mol. Biol.* **228**, 862–869.
34. Davis, J.P., Janjić, N., Pribnow, D. & Zichi, D. A. (1995). Alignment editing and identification of consensus secondary structures for nucleic acid sequences. Interactive use of dot matrix representations. *Nucleic Acids Res.*, in press.
35. States, D.J. & Boguski, M.S. (1992). Similarity and homology. In *Sequence Analysis Primer*, pp 89–157, Freeman, New York.
36. Pieken, W.A., Olsen, D.B., Benseler, F., Aurup, H. & Eckstein, F. (1991). Kinetic characterization of ribonuclease-resistant 2'-modified hammerhead ribozymes. *Science* **253**, 314–317.
37. Hobbs, J., Sternbach, H., Sprinzl, M. & Eckstein, F. (1973). Polynucleotides containing 2'-amino-2'-deoxyribose and 2'-azido-2'-deoxyribose. *Biochemistry* **12**, 5138–5145.
38. Miller, P S., Bhan, P. & Kan, L.-S. (1993). Synthesis and interactions of oligodeoxyribonucleotides containing 2'-amino-2'-deoxyuridine. *Nucleosides Nucleotides* **12**, 785–792.
39. Aurup, H., Tuschl, T., Benseler, F., Ludwig, J. & Eckstein, F. (1994). Oligonucleotide duplexes containing 2'-amino-2'deoxycytidines: thermal stability and chemical reactivity. *Nucleic Acids Res.* **22**, 20–24.
40. Inoue, H., Hayase, Y., Imura, A., Iwai, S., Kazunobu, M. & Ohtsuka, E. (1987). Synthesis and hybridization studies on two complementary nona(2'-O-methyl)ribonucleotides. *Nucleic Acids Res.* **15**, 6131–6148.
41. Lesnik, E.A., *et al.*, & Freier, S.M. (1993). Oligodeoxynucleotides containing 2'-O-modified adenosine: Synthesis and effects on stability of DNA:RNA duplexes. *Biochemistry* **32**, 7832–7838.
42. Schneider, T.D., Stormo, G.D., Gold, L. & Ehrenfeucht, A. (1986). Information content of binding sites on nucleotide sequences. *J. Mol. Biol.* **188**, 415–431.
43. Jellinek, D., Lynott, C.K., Rifkin, D.B. & Janjić, N. (1993). High-

affinity RNA ligands to basic fibroblast growth factor inhibit receptor binding. *Proc. Natl. Acad. Sci. USA* **90**, 11227–11231.
44. Green, L., Waugh, S., Binkley, J.P., Hostomska, Z., Hostomsky, Z. & Tuerk, C. (1995). Comprehensive chemical modification interference analysis of an RNA pseudoknot inhibitor to HIV-1 reverse transcriptase. *J. Mol. Biol.* **247**, 60–68.
45. Fersht, A. (1985). Measurement and magnitude of enzymatic rate constants. In *Enzyme Structure and Mechanism*. pp. 121–154, Freeman, New York.
46. Long, K.S. & Crothers, D.M. (1995). Interaction of human immunodeficiency virus type 1 Tat-derived peptides with TAR RNA. *Biochemistry* **34**, 8885–8895.
47. Jakeman, L.B., Winer, J., Bennett, G.L., Altar, C.A. & Ferrara, N. (1992). Binding sites for vascular endothelial growth factor are localized on endothelial cells in adult rat tissues. *J. Clin. Invest.* **89**, 244–253.
48. Moscatelli, D. (1992). Basic fibroblast growth factor (bFGF) dissociates rapidly from heparan sulfates but slowly from receptors. *J. Biol. Chem.* **267**, 25803–25809.
49. Raines, E.W., Bowen-Pope, D.F. & Ross, R. (1991). Platelet-derived growth factor. In *Peptide Growth Factors and Their Receptors*. (Sporn, M.B. & Roberts, A.B., eds), pp. 173–262, Springer-Verlag, New York.
50. Milligan, J.F. & Uhlenbeck, O.C. (1989). Determination of RNA–protein contacts using thiophosphate substitutions. *Biochemistry* **28**, 2849–2855.
51. Lowary, P. & Uhlenbeck, O.C. (1987). An RNA mutation that increases the affinity of an RNA–protein interaction. *Nucleic Acids Res.* **15**, 10483–10493.
52. Abbas, A.K., Lichtman, A.H. & Pober, J.S. (1994). Maturation of B lymphocytes and expression of immunoglobulin genes. In *Cellular and Molecular Immunology*. (2nd Edn), pp. 66–95, Saunders, Philadelphia, PA.
53. McGee, D.P.C., Vargeese, C., Zhai, Y., Kirchenheuter, G.P., Siedem, C.R. & Pieken, W.A. (1995). Efficient synthesis of 2'-amino-2'-deoxypyrimidine 5'-triphosphates. *Nucleosides Nucleotides*, in press.
54. Sinha, D.N., Biernat, J., McManus, J. & Koester, H. (1984). Polymer support oligonucleotide synthesis XVIII: use of β-cyanoethyl-N, N-dialkylamino-N-morpholino phosphoramidite of deoxynucleotides for the synthesis of DNA fragments. *Nucleic Acids Res.* **12**, 4539–4557.
55. Scaringe, S.A., Francklyn, C. & Usman, N. (1990). Chemical synthesis of biologically active oligoribonucleotides using β-cyanoethyl protected ribonucleotide phosphoramidites. *Nucleic Acids Res.* **18**, 5433–5441.
56. Imazawa, I. & Eckstein, F. (1979). Facile synthesis of 2'-amino-2'-deoxyribofuranosyl purines. *J. Org. Chem.* **44**, 2039–2041.
57. Milligan, J.F., Groebe, D.R., Witherell, G.W. & Uhlenbeck, O.C. (1987). Oligoribonucleotide synthesis using T7 RNA polymerase and synthetic DNA templates. *Nucleic Acids Res.* **15**, 8783–8798.
58. Hore, P.J. (1983). A new method for water suppression in the protein NMR spectra of aqueous solutions. *J. Magn. Reson.* **54**, 539–542.

Received: **6 Sep 1995**; revisions requested: **26 Sep 1995**; revisions received: **29 Sep 1995**. Accepted: **3 Oct 1995**.